Preparation, Crystal Structures, and Properties of the Acetate-Bridged Platinum(III) Compounds $[\{(H_2O)Pt(\mu\text{-}CH_3CO_2)_2\}_2]A_2$ ($A^- = ClO_4^-$, $CF_3SO_3^-$)[1]

Trevor G. Appleton,* Karl A. Byriel, Jodie M. Garrett, John R. Hall, Colin H. L. Kennard, Michael T. Mathieson, and Robert Stranger

Chemistry Department, The University of Queensland, Brisbane, Qld., Australia 4072

Received February 15, 1995[⊗]

Reaction of $K_2[Pt(NO_2)_4]$ with $CH_3CO_2H/H_2O/HA$, where HA = $HClO_4$, CF_3SO_3H, or HNO_3, gave $[\{(H_2O)Pt(\mu\text{-}CH_3CO_2)_2\}_2]A_2$. With nitrite highly enriched in ^{15}N, the reactions which led to these final products were followed by ^{195}Pt NMR, and intermediate platinum(III) complexes were identified. Crystal structures were determined by X-ray diffraction for the perchlorate and trifluoromethanesulfonate salts: for $[\{(H_2O)Pt(\mu\text{-}CH_3CO_2)_2\}_2](ClO_4)_2$, monoclinic crystal system, space group $P2_1/c$, $a = 8.113(4)$ Å, $b = 8.279(2)$ Å, $c = 14.892(7)$ Å, $\beta = 101.16(2)°$, $V = 981.4(7)$ Å^3, $Z = 2$, Pt−Pt = 2.3906(13) Å; for $[\{(H_2O)Pt(\mu\text{-}CH_3CO_2)_2\}_2](CF_3SO_3)_2\cdot 4H_2O$, monoclinic crystal system, space group $P2_1/c$, $a = 8.162(2)$ Å, $b = 8.982(1)$ Å, $c = 19.404(6)$ Å, $\beta = 95.51(1)°$, $V = 1416.0(5)$ Å^3, $Z = 2$, Pt−Pt = 2.3929(6) Å. In water, there was rapid conversion to a complex with three acetate bridges. In acetic acid or dmf, there was replacement of the axial water ligands by acetate or dmf, respectively, but the tetra-acetate-bridged structure remained intact for several hours. Some axially-substituted derivatives were obtained in solution by addition of ligands to a dmf solution of the trifluoromethanesulfonate salt and were characterized by ^{195}Pt NMR. Solids $[\{XPt(\mu\text{-}CH_3CO_2)_2\}_2]$ were isolated with X = Cl, Br. The crystal structures of $[\{(H_2O)Pt(\mu\text{-}CH_3CO_2)_2\}_2]A_2$ showed Pt−Pt−O(acetate) angles slightly less than 90°. This, together with very low shielding of the carboxylate carbon nuclei in the tetra-acetate-bridged complexes, was interpreted as indicating strain in these structures. UV spectra of the compounds were similar to those of sulfate- and hydrogen phosphate-bridged platinum(III) complexes with the same axial ligands.

Introduction

Many metal ions form dinuclear acetates, in which the two metal ions are bridged by four acetate ligands, to give a "lantern structure".[2] Among the best-known of these complexes is the rhodium(II) acetate $[\{(H_2O)Rh(\mu\text{-}CH_3CO_2)_2\}_2]$, for which the crystal structure was first determined in 1962,[3] with a more accurate determination subsequently.[4,5] It is now well-accepted[6,7] that this complex contains a single Rh−Rh bond which can be represented as $\sigma^2\pi^4\delta^2\delta^{*2}\pi^{*4}$.

Electronically analogous platinum(III) complexes $[\{(H_2O)Pt(\mu\text{-}SO_4)_2\}_2]^{2-}$ [8,9] and $[\{(H_2O)Pt(\mu\text{-}PO_4H)_2\}_2]^{2-}$ [9-11] are now well-characterized. They may be obtained by reaction of $K_2[Pt(NO_2)_4]$ with H_2SO_4 and H_3PO_4, respectively.[8,12,13] As described elsewhere,[14] we studied the reactions of $K_2[Pt(NO_2)_4]$ with acetic acid/water under various conditions. Platinum(III) complexes containing both nitrite-*N* and acetate as ligands were among the products of these reactions, but no nitrite-free compound was detected. However, we also showed[14] that all of the nitrite could be removed from platinum(II) by treatment under oxidizing conditions with a strong acid HA, perchloric or trifluoromethanesulfonic ("triflic") acid. It therefore occurred to us that a possible route to the desired acetate-bridged platinum(III) compound was by reaction of $K_2[Pt(NO_2)_4]$ with a $CH_3CO_2H/H_2O/HA$ mixture. This paper describes the preparation in this manner of the compounds $[\{(H_2O)Pt(\mu\text{-}CH_3CO_2)_2\}_2]A_2$ (salts of the cation, **1**, $A^- = ClO_4^-$, $CF_3SO_3^-$, NO_3^-), the crystal structures of the perchlorate and triflate salts (determined by X-ray diffraction), and a spectroscopic (NMR, UV, IR) study of these compounds and some axially-substituted derivatives.

Experimental Section

Starting Materials. $K_2[Pt(NO_2)_4]\cdot 2H_2O$, with either [$^{14}N$]- or [$^{15}N$]-nitrite, was prepared as previously described.[15] Sodium nitrite highly enriched in ^{15}N (>98%) (CIL) was supplied by Novachem (Melbourne, Australia).

NMR Spectra. The 21.4-MHz ^{195}Pt NMR spectra (^{195}Pt, $I = 1/2$, 33.6% abundance) were obtained with the use of a JEOL FX-100 instrument, as previously described.[15] The 200.1-MHz ^1H, 50.3-MHz ^{13}C, and 20.3-MHz ^{15}N NMR spectra were obtained with the use of a Bruker AC-200F spectrometer, as previously described.[15,16] The 75.5-MHz solid state ^{13}C spectra were provided by the Centre for Magnetic

* Author to whom correspondence should be addressed.

[⊗] Abstract published in *Advance ACS Abstracts,* September 15, 1995.

(1) A preliminary account of some of these results has been published: Appleton, T. G.; Byriel, K. A.; Hall, J. R.; Kennard, C. H. L.; Mathieson, M. T. *J. Am Chem. Soc.* **1992**, *114*, 7305.
(2) Cotton, F. A.; Walton, R. A. *Struct. Bonding* **1985**, *62*, 1.
(3) Porai-Koshits, M. A.; Antsyshkina, A. S. *Dokl. Akad. Nauk SSSR* **1962**, *146*, 1102.
(4) Cotton, F. A.; DeBoer, B. G.; La Prade, M. D.; Pipal, J. R.; Ucko, D. A. *J. Am. Chem. Soc.* **1970**, *92*, 2926.
(5) Cotton, F. A.; DeBoer, B. G.; La Prade, M. D.; Pipal, J. R.; Ucko, D. A. *Acta Crystallogr.* **1971**, *B27*, 1664.
(6) Dubicki, L.; Martin, R. L. *Inorg. Chem.* **1970**, *9*, 673.
(7) Norman, J. G.; Kolari, H. J. *J. Am. Chem. Soc.* **1978**, *100*, 791.
(8) Muraveiskaya, G. S.; Kukina, G. A.; Orlova, V. S.; Evstaf'eva, O. N.; Porai-Koshits, M. A. *Dokl. Akad. Nauk SSSR* **1976**, *226*, 596.
(9) Bancroft, D. P.; Cotton, F. A.; Falvello, L. R.; Han, S.; Schwotzer, W. *Inorg. Chim. Acta* **1984**, *87*, 147.
(10) Muraveiskaya, G. S.; Abashkin, V. E.; Evstaf'eva, N.; Golovaneva, I. F.; Schchelokov, R. N. *Koord. Khim.* **1980**, *6*, 463.
(11) Cotton, F. A.; Falvello, L. R.; Han, S. *Inorg. Chem.* **1982**, *21*, 1709.
(12) Muraveiskaya, G. S.; Orlova, V. S.; Evstaf'eva, O. N. *Zh. Neorg. Khim.* **1977**, *22*, 1319.
(13) Appleton, T. G.; Hall, J. R.; Neale, D. W. *Inorg. Chim. Acta* **1985**, *104*, 19.
(14) Appleton, T. G.; Barnham, K. J.; Byriel, K. A.; Hall, J. R.; Kennard, C. H. L.; Mathieson, M. T.; Penman, K. G. *Inorg. Chem.*, in press.
(15) Appleton, T. G.; Barnham, K. J.; Hall, J. R.; Mathieson, M. T. *Inorg. Chem.* **1991**, *30*, 2751.
(16) Appleton, T. G.; Bailey, A. J.; Bedgood, D. R.; Hall, J. R. *Inorg. Chem.* **1994**, *33*, 217.

0020-1669/95/1334-5646$09.00/0

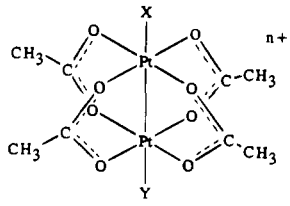

1	X = Y = H_2O	n = 2
9	X = Y = -O_2CCH_3	n = 0
15	X = Y = dmf	n = 2
16	X = dmf, Y = H_2O	n = 2
17	X = Y = Cl	n = 0
18	X = Y = Br	n = 0
19	X = Cl, Y = dmf	n = 1
20	X = Y = py	n = 2
21	X = py, Y = dmf	n = 2
22	X = Y = SEt_2	n = 2
23	X = SEt_2, Y = dmf	n = 2

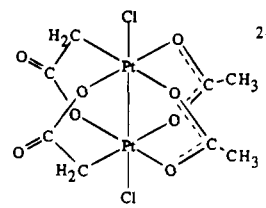

24

Resonance at the University of Queensland, with the use of a Bruker MSL-300 instrument equipped with a 7-mm cross-polarization/magic angle spinning (CP/MAS) probe, with high-power proton decoupling. The samples were packed as crystalline powders into standard 7-mm rotors. Ambient probe temperature was 297 K. The cross-polarization contact time was 5 ms, probe dead time 15 μs, acquisition time 13 ms, recycle delay 6 s, pulse width (π/2) 3.4 μs, sweep width 38 460 Hz, number of data points 1K (zero-filled to 8K when data were manipulated), line broadening 20−50 Hz, number of scans 50−500, and spinning rate 2.5−3.0 kHz.

All spectra other than ^{1}H spectra were ^{1}H-decoupled. Shifts are positive to higher frequency. The ^{195}Pt NMR spectra are referenced relative to a separate sample containing 0.5 g of $Na_2[PtCl_6]$ in 2 mL of H_2O (δ_{Pt} = 0), and ^{15}N NMR spectra to the $^{15}NH_4^+$ signal from a 5 M solution of $(^{15}NH_4)_2SO_4$ in 1 M H_2SO_4 in a coaxial capillary (δ_N = 0). The ^{13}C and ^{1}H peaks in organic solvents were referenced relative to internal tetramethylsilane (TMS), and ^{1}H peaks in D_2O were referenced to the methyl signal of sodium trimethylsilylpropane-3-sulfonate (TSS).

Other Instrumentation and Procedures. Solution electronic spectra were recorded with a single-beam Beckman DU-7500 spectrophotometer using quartz cells (1-cm path length), at 296 K. Some spectra were run on the complex cation bound to Nafion film (Nafion 117 film, 0.007 in. thick). This is a sulfonated poly(perfluoroethylene). A square of Nafion film (approximately 1 cm × 1 cm) was dipped into a freshly-prepared solution of $[\{(H_2O)Pt(\mu\text{-}CH_3CO_2)_2\}_2](CF_3SO_3)_2$ in *N,N*-dimethylformamide (dmf) (10^{-2} M) for approximately 1 s.

IR spectra were run either on KBr pellets or on Nujol and hexachlorobutadiene mulls between KBr disks, on a Perkin-Elmer 1600 FTIR spectrometer.

Some C,H,N microanalyses were carried out by the microanalytical service in this department. Analyses for halides and some C,H,N analyses were performed by the National Analytical Laboratories Pty Ltd., Melbourne. All substances isolated gave satisfactory microanalyses.

Preparation of $[\{(H_2O)Pt(\mu\text{-}CH_3CO_2)_2\}_2](ClO_4)_2$. *Caution! This perchlorate salt is potentially explosive. On two separate occasions, very small quantities detonated. Small quantities only should be prepared and precautions taken during handling.* To $K_2[Pt(NO_2)_4]\cdot 2H_2O$ (0.50 g, 1.01 mmol) in a 50-mL round-bottomed flask was added 15 mL of a 2:1 (by volume) mixture of glacial acetic acid and 1 M aqueous perchloric acid solution. The stirred mixture was heated at 90−100 °C for 3 h, with a gentle stream of air bubbling through. Additions of small volumes of the acetic acid/$HClO_4$/H_2O mixture were made from time to time, to maintain the volume at 10−15 mL. The reaction mixture was then cooled in an ice bath for 20 min, and the solid $KClO_4$ which deposited was filtered off. The filtrate was heated, under conditions similar to those already described, for a further 3−4 h. A small quantity of yellow crystals was present at this stage. The volume was then decreased to 5 mL by continued heating with air bubbling through the mixture, which was then cooled in ice. The yellow solid was separated from the mixture by centrifugation, washed with two 2-mL portions of *ice cold* acetic acid/perchloric acid solution, two 2-mL portions of *ice cold* ethanol, and then two 5-mL portions of diethyl ether, and pumped dry under vacuum. The yield at this stage was 0.24 g (55%). A second crop could be obtained by concentrating the mother liquor further.

Table 1. Crystallographic Data for $[\{(H_2O)Pt(\mu\text{-}CH_3CO_2)_2\}_2](ClO_4)_2$ and $[\{(H_2O)Pt(\mu\text{-}CH_3CO_2)_2\}(CF_3SO_3)_2\cdot 4H_2O$

	perchlorate	trifluoromethanesulfonate
chem formula	$C_8H_{16}Cl_2O_{18}Pt_2$	$C_{10}H_{24}F_6O_{20}Pt_2S_2$
fw	861.3	1032.6
space group	$P2_1/c$ (No. 14)	$P2_1/c$ (No. 14)
a (Å)	8.113(4)	8.162(2)
b (Å)	8.279(2)	8.982(1)
c (Å)	14.892(7)	19.404(6)
β (deg)	101.16(2)	95.51(1)
V (Å^3)	981.4(7)	1416.0(5)
Z	2	2
T (K)	298	298
λ (Å)	0.710 73	0.710 73
ρ_{calcd} (g cm^{-3})	2.915	2.422
μ (cm^{-1})	146.0	101.35
R	0.0456	0.0218
R_w	0.1138	0.0542

Preparation of $[\{(H_2O)Pt(\mu\text{-}CH_3CO_2)_2\}_2](CF_3SO_3)_2$. To $K_2[Pt(NO_2)_4]\cdot 2H_2O$ (1.00 g, 2.03 mmol) was added 15 mL of a 2:1 (by volume) mixture of glacial acetic acid/1 M trifluoromethanesulfonic acid solution in water. The resultant mixture was heated in an oil bath at 130 °C, with stirring and with a gentle stream of air passing through. The solution volume was maintained at 10−15 mL for 4 h by periodic additions of the acid/solvent mixture, and then the volume was allowed to decrease until a copious amount of an orange solid was present. (A darker, oily solid formed if there had been insufficient heating. If this happened, more solvent was added, and heating was resumed). The mixture was then cooled in ice. The solid was isolated by centrifugation and washed with two 2-mL portions each of *ice cold* water, *ice cold* ethanol, and diethyl ether. Crystals to be used for structure determination were selected at this stage, when lattice water ($\cdot 4H_2O$) was present. The bulk solid was dried under vacuum, which caused loss of the lattice water. The yield was 0.80 g (82%).

Preparation of $[\{(H_2O)Pt(\mu\text{-}CH_3CO_2)_2\}_2](NO_3)_2$. This preparation was similar to that used for the perchlorate salt, with 1 M nitric acid used in place of perchloric acid. As with the perchlorate, intermediate cooling was necessary, with removal of deposited KNO_3. The yield was variable, partly because concentration of the mother liquor after the first crop of solid gave a product contaminated with KNO_3. In some preparations, some $K_2[Pt(NO_2)_6]$ was also produced. The best yield of the nitrate salt from 0.50 g of $K_2[Pt(NO_2)_4]\cdot 2H_2O$ was 0.12 g (30%).

Preparations of $[\{XPt(\mu\text{-}CH_3CO_2)_2\}_2]$ (X = Cl, Br). To prepare the chloro complex, solid $[\{(H_2O)Pt(\mu\text{-}CH_3CO_2)_2\}_2](CF_3SO_3)_2$ (0.25 g, 0.26 mmol) was added in small portions, with stirring, to a solution of lithium chloride (0.023 g, 0.54 mmol) in 0.5 mL of dmf. Stirring was continued for 5−10 min, during which time a yellow solid precipitated. The solid was separated from the mother liquor by centrifugation (this was carried out without undue delay, to avoid contamination of the product with decomposition products). It was then washed thoroughly with cold water, ethanol, and diethyl ether and dried under vacuum. The yield was 0.31 g (72%).

The dibromo complex was prepared in a similar way, with lithium bromide used instead of LiCl. The yield was 30%. The solid slowly decomposed on standing at ambient temperature.

Crystal Structure Determinations for the Perchlorate and Trifluoromethanesulfonate Salts of $[\{(H_2O)Pt(\mu\text{-}CH_3CO_2)_2\}_2]^{2+}$. Intensity data were collected at 298 K with the use of an Enraf-Nonius CAD4 diffractometer, with graphite-monochromatized Mo Kα (λ = 0.710 73 Å) radiation. Details of data collection for the two compounds are provided in Table 1. Crystallographic data were collected with a package program provided by Enraf-Nonius, Delft, The Netherlands. The platinum positions were determined from a Patterson synthesis,[17] and the remaining non-hydrogen atoms were located from a difference

(17) Sheldrick, G. M. SHELXS-86, Structure Solution Package. University of Göttingen, Germany, 1986.

Scheme 1

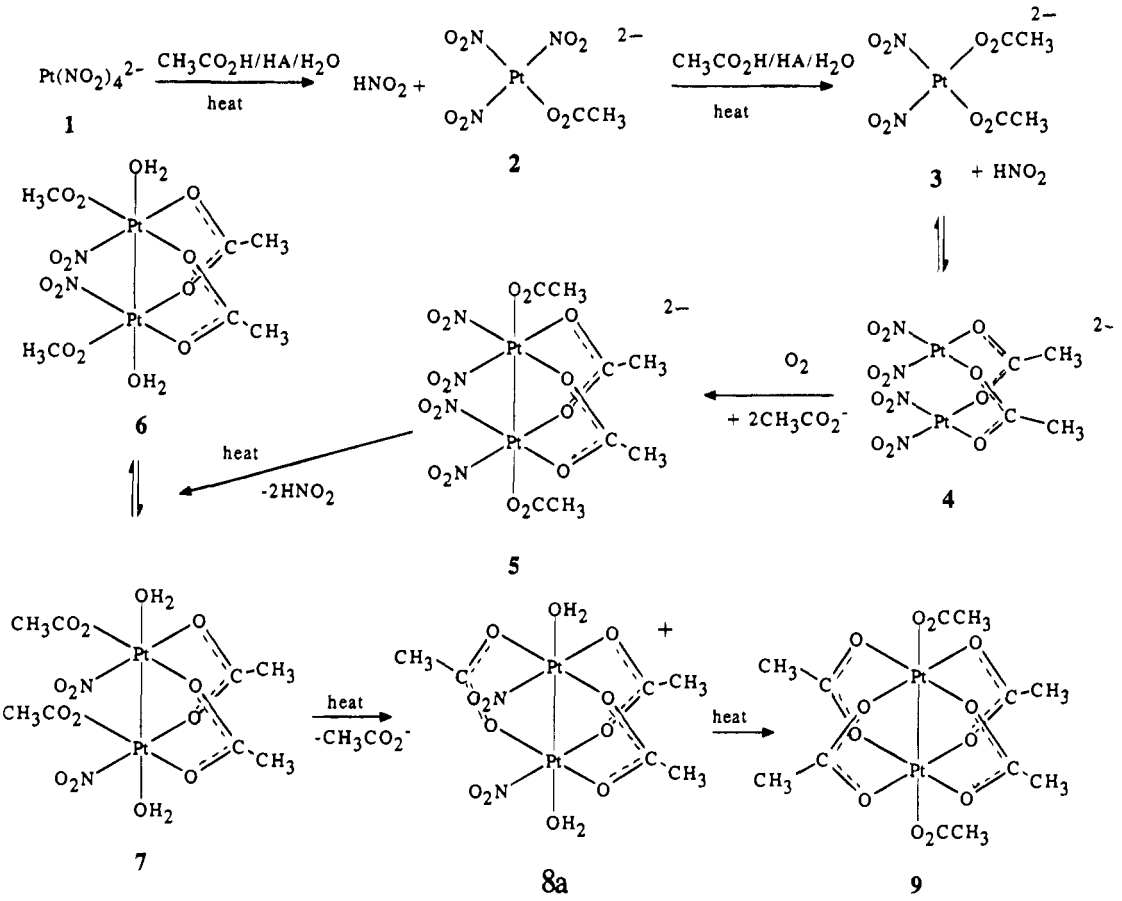

synthesis.[18] Atom positional and anisotropic thermal parameters were refined using least squares.

Monitoring of the Reaction between $K_2[Pt(NO_2)_4]$ and CH_3CO_2H/HA by NMR. $K_2[Pt(^{15}NO_2)_4]\cdot 2H_2O$ (0.25g) was dissolved in a 2:1 (by volume) CH_3CO_2H/1 M HA mixture (HA = $HClO_4$ or CF_3SO_3H) (10 mL) in a Schlenk tube, and the resultant mixture was heated at 90−100 °C by immersion in an oil bath, with a gas (O_2 or Ar) either bubbling through the solution or providing the atmosphere above the solution. The volume was kept between 5 and 10 mL by regular addition of aliquots of the reaction solvent. From time to time, the tube was removed from the oil bath, effectively quenching the reaction. An aliquot (2 mL) of the reaction mixture was removed, examined by ^{195}Pt NMR, and then returned to the reaction vessel. Heating was then resumed. When the reaction was carried out under argon, the solution was degassed by a freeze−thaw technique before heating began.

Results

Preparation of $[\{(H_2O)Pt(\mu\text{-}CH_3CO_2)_2\}_2]A_2$ (Scheme 1). The reactions of $K_2[Pt(NO_2)_4]$ with CH_3CO_2H/HA/H_2O (HA = $HClO_4$, CF_3SO_3H, HNO_3) did lead to the desired compounds, $[\{(H_2O)Pt(\mu\text{-}CH_3CO_2)_2\}_2]A_2$ ([**1**]A_2), which crystallized from the reaction mixture after cooling. The same final product was obtained whether the reaction was carried out under oxygen or under argon, but the reactions were faster when oxygen was present. The details given in the Experimental Section therefore describe the preparation under oxygen. We have shown[14,15] that ^{195}Pt NMR is a powerful technique for the characterization in solution of platinum complexes containing nitrite, especially when the nitrite ligands are highly enriched in ^{15}N. The reaction of $K_2[Pt(^{15}NO_2)_4]$ with 2:1 CH_3CO_2H/1 M $HClO_4$ was therefore followed by ^{195}Pt NMR, both under oxygen and under argon. The characteristic ^{195}Pt NMR patterns obtained for a number of ([^{15}N]nitrito)platinum(III) complexes have been previously described.[14] The analysis of these patterns will therefore not be described again in detail here.

Under oxygen or argon, the initially colorless solution of $K_2[Pt(^{15}NO_2)_4]$ in the CH_3CO_2H/$HClO_4$/H_2O solvent became deep blue (λ_{max} 618 nm) when heating commenced and then, with continued heating, green, yellow, and orange. These color changes paralleled those previously observed for reaction with $HClO_4/H_2O$.[14] The blue color is due to nitrosylplatinum(IV) complexes.[14,19] No ^{195}Pt signals could be detected from blue or green solutions containing these paramagnetic species. The species identified by NMR in the reaction under oxygen are shown in Scheme 1, and ^{195}Pt NMR spectra (in the "Pt(III) region") after different heating times are shown in Figure 1. The ^{195}Pt NMR spectrum of the yellow solution obtained after 30 min showed peaks (not illustrated) due to the platinum(II) complexes $[Pt(^{15}NO_2)_3(O_2CCH_3)]^{2-}$ (**2**) and *cis*-$[Pt(^{15}NO_2)_2(O_2CCH_3)_2]^{2-}$ (**3**).[14,15] We have previously shown[14] that **2** exists in equilibrium with a small proportion of the dinuclear platinum(II) complex with acetate bridges $[\{Pt(^{15}NO_2)_2(\mu\text{-}CH_3CO_2)\}_2]^{2-}$(**4**).

The ^{195}Pt NMR spectrum of this solution in the platinum(III) region is shown in Figure 1a. The pattern, centered at 1027 ppm, has the appearance of a 1:2:1 triplet with an additional two lines between the lines of the triplet. As we have discussed previously,[14] this pattern arises from the superposition of a triplet on a quintet and is characteristic of the platinum(III) complex $[\{(CH_3CO_2)Pt(^{15}NO_2)_2(\mu\text{-}CH_3CO_2)\}_2]^{2-}$ (**5**). The analogous complex with axial water ligands gives a similar pattern at 874 ppm,[14] which was not detected in this spectrum.

With further heating, the peaks from **5** decreased in intensity,

(18) Sheldrick, G. M. SHELX-76, Program for Crystal Structure Determination. Cambridge University, U.K., 1976.

(19) Peterson, E. S.; Larsen, R. D.; Abbott, E. H. *Inorg. Chem.* **1988**, *27*, 3514.

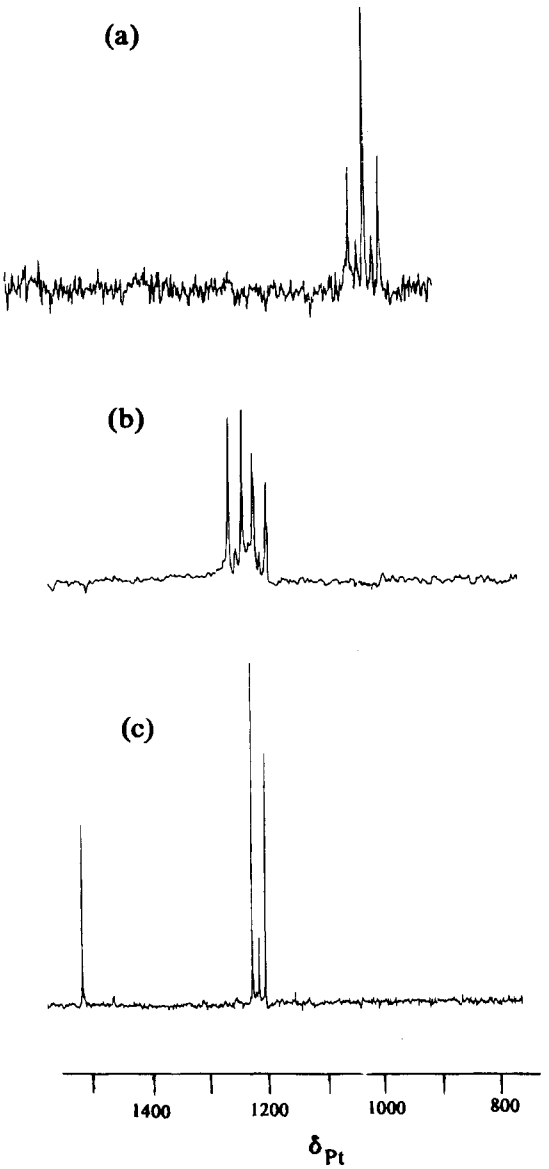

Figure 1. 21.4-MHz ^{195}Pt NMR spectra in the platinum(III) region of a solution of $K_2[Pt(^{15}NO_2)_4]$ heated at 90−100 °C in 2:1 CH_3CO_2H/1 M $HClO_4$ for (a) 30, (b) 270, and (c) 420 min.

to be replaced by a number of patterns, each resembling a doublet with a small singlet in the center of the doublet (Figure 1b,c). As previously discussed,[14] such a pattern arises from superposition of a doublet on a 1:2:1 triplet and is characteristic of a symmetrical dinuclear platinum(III) species with one [^{15}N]nitrite bound to each platinum atom. The spectrum after a total heating time of 7 h (Figure 1c) showed only one "doublet plus triplet" pattern, at 1215 ppm (as well as a singlet at 1510 ppm).

In the reaction of $K_2[Pt(^{15}NO_2)_4]$ with 3:1 CH_3CO_2H/H_2O, after prolonged heating, a "doublet plus triplet" pattern was observed at 1315 ppm, which was assigned to $[\{(CH_3CO_2)Pt(^{15}NO_2)\}_2(\mu\text{-}CH_3CO_2)_3]^-$ (**8b**).[14] This Pt shift is 100 ppm away from that of the "doublet plus triplet" observed after heating a 2:1 CH_3CO_2H/1 M $HClO_4$ solution for 7 h (1215 ppm, Figure 1c). Solvent effects can clearly affect δ_{Pt} of Pt(III) complexes up to approximately 30 ppm,[14] but this difference appeared to be too large to be explained on this basis. A separate sample was prepared with a significantly increased proportion of acetic acid present (3:1 by volume CH_3CO_2H/1 M $HClO_4$, rather than 2:1). The ^{195}Pt NMR spectrum showed a "doublet plus triplet" pattern at 1225 ppm (J(Pt−N) 491 Hz). The 10 ppm difference in δ_{Pt} from that in the spectrum shown in Figure 1c could be ascribed to the difference in solvent composition. An excess of sodium acetate was added (0.6 g of $Na(CH_3CO_2)\cdot 3H_2O$ added to 3 mL of solution). The ^{195}Pt NMR spectrum of the resultant solution showed a "doublet plus triplet" pattern at 1342 ppm (J(Pt−N) 515 Hz). Allowing for the effect on δ_{Pt} of the perchloric acid and excess sodium acetate present, this pattern could be identified with that previously observed at 1315 ppm in 3:1 acetic acid/water, assigned to $[\{(CH_3CO_2)Pt(^{15}NO_2)\}_2(\mu\text{-}CH_3CO_2)\}_3]^-$ (**8b**). The species observed in the acetic acid/perchloric acid solutions would therefore be $[\{(H_2O)Pt(^{15}NO_2)\}_2(\mu\text{-}CH_3CO_2)_3]^+$ (**8a**), related to **8b** by eq 1. It is interesting that **8a**, with axial water substitution,

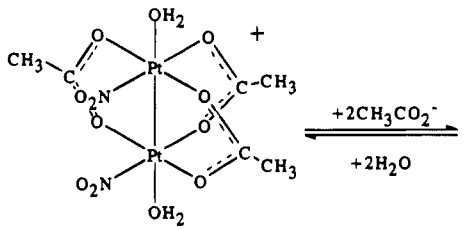

8a

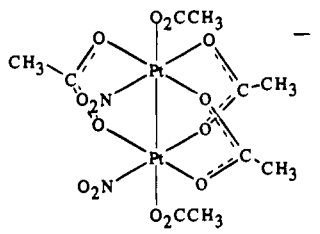

8b

(1)

was present in this solvent. At other stages of the reaction, compounds with axial acetate, $[\{(CH_3CO_2)Pt(NO_2)_2(\mu\text{-}CH_3CO_2)\}_2]^{2-}$ (**5**) and $[\{(CH_3CO_2)Pt(\mu\text{-}CH_3CO_2)_2\}_2]$ (**9**) (see below), were present in solvents with the same composition. The equilibrium constant for formation of the axial diacetato complex must be lower for the **8a/b** pair, so that protonation by $HClO_4$ causes the equilibrium to shift to the axial diaqua complex **8a** in the acetic acid/perchloric acid medium.

For the 2:1 acetic acid/1 M $HClO_4$ solution which had been heated for less time, ^{195}Pt spectra were obtained which showed other "doublet plus triplet" patterns. For example, the spectrum after a total heating time of 4.5 h (Figure 1b), showed two "doublet plus triplet" patterns, at 1250 and 1207 ppm (each with J(Pt−N) 484 Hz) (as well as a weak signal from **8a** at 1215 ppm). Species that could give rise to these signals include the isomers of $[\{(H_2O)Pt(^{15}NO_2)(O_2CCH_3)(\mu\text{-}CH_3CO_2)\}_2]$, **6** and **7** (Scheme 1), but other possibilities include analogous complexes with "equatorial" aqua ligands, $[\{(H_2O)Pt(^{15}NO_2)(H_2O)(\mu\text{-}CH_3CO_2)\}_2]^{2+}$.

The ^{195}Pt spectrum after the solution was heated 7 h showed, in addition to the "doublet plus triplet" assigned to **8a**, a singlet at 1510 ppm. A singlet pattern indicated a species with no [^{15}N]nitrite bound to platinum. The same peak was observed in the ^{195}Pt NMR spectrum when a salt of $[\{(H_2O)Pt(\mu\text{-}CH_3CO_2)_2\}_2]^{2+}$ (**1**) was dissolved in glacial acetic acid (see below) and was assigned to $[\{(CH_3CO_2)Pt(\mu\text{-}CH_3CO_2)_2\}_2]$ (**9**). With continued heating, this singlet increased in intensity, and $[\mathbf{1}](ClO_4)_2$ crystallized from a solution after concentration.

Remarkably, the ^{195}Pt NMR spectra of these solutions showed no peaks due to platinum(IV) complexes when mixtures of acetic with perchloric or triflic acid were used. Reactions under similar conditions with CH_3CO_2H/H_2O always produced significant amounts of platinum(IV) compounds.[14] When HNO_3 was used

Scheme 2

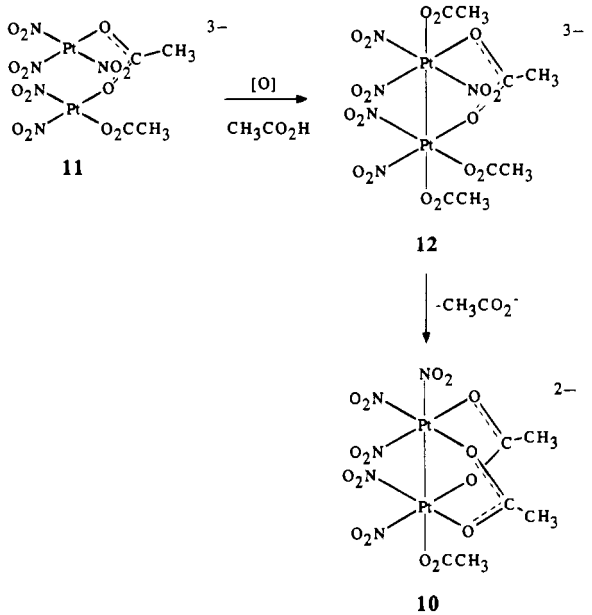

as the strong acid, mixed with acetic acid, however, a signal due to $[Pt(NO_2)_6]^{2-}$ was observed at 2627 ppm.

Reactions of $K_2[Pt(NO_2)_4]$ with 2:1 CH_3CO_2H/1 M $HClO_4$ under argon proceeded by a different route to the same end product. The initial blue color faded through green to yellow within 30 min, and the ^{195}Pt NMR spectrum in the platinum(III) region showed peaks due to both $[\{(CH_3CO_2)Pt(NO_2)_2(\mu\text{-}CH_3CO_2)\}_2]^{2-}$ (**5**) and the unsymmetrical complex[14] $[(NO_2)Pt(NO_2)_2(\mu\text{-}CH_3CO_2)_2Pt(NO_2)_2(CH_3CO_2)]^{2-}$ (**10**). With continued heating, the ^{195}Pt NMR resonance due to **10** decreased in intensity, while that from **5** increased. The "doublet plus triplet" assigned to **8a** and the singlet from **9** then slowly appeared in their place. Again, no peaks from platinum(IV) complexes were present.

We have shown[14] that **10** may be formed from reaction of $[\{Pt^{II}(NO_2)_2(\mu\text{-}CH_3CO_2)\}_2]^{2-}$ (**4**) with NO_2, but under the present anaerobic conditions, no NO_2 would have been present. We have also suggested[14] that **10** may be formed *via* the oxidation of a dinuclear species such as **11** (Scheme 2). Under anaerobic conditions, oxidation would be primarily by HNO_3 generated by decomposition of HNO_2. Oxidation would be slower than in the presence of dioxygen, but so too would be the removal of coordinated nitrite. When removal of coordinated nitrite is slow overall compared with oxidation, the reactions shown in Scheme 2 would be favored.

In the final spectra obtained from reactions under both oxygen and argon conditions, there were a number of very weak singlets (in addition to the large peak from **9**) that would be due to nitrite-free platinum(III) complexes. No attempt was made to assign these weak peaks to particular compounds, but the complex with axial aqua ligands, **1**, was presumably among those present in solution in low concentration. The crystallization of the salts $[\mathbf{1}]A_2$ from the reaction mixtures therefore was driven by the low solubilities of these salts in the reaction media, rather than high concentrations of **1** in solution.

The IR spectrum of the triflate salt showed, as well as the expected peaks from the anion, bands characteristic of the bridging acetate ligands (CO_2^-: ν_{as} 1562 cm^{-1}, ν_s 1422 cm^{-1}) and axial water ligands (3530 cm^{-1}).

Structures of the Perchlorate and Triflate Salts of $[\{(H_2O)Pt(\mu\text{-}CH_3CO_2)_2\}_2]^{2+}$ (1). Atomic coordinates and thermal parameters for the two structures are given in Tables 2 and 3, respectively. Both structures contain the cation **1**, with no

Table 2. Final Coordinates ($\times 10^4$) and Equivalent Isotropic Displacement Parameters ($Å^2 \times 10^3$) for Non-Hydrogen Atoms in $[\{(H_2O)Pt(\mu\text{-}CH_3CO_2)_2\}_2](ClO_4)_2$

	x	y	z	U(eq)[a]
Pt(1)	602(1)	1322(1)	87(1)	24(1)
O(1)	1698(15)	3725(16)	299(8)	38(3)
C(10)	−836(21)	140(22)	2610(10)	32(4)
C(11)	−516(19)	93(21)	1655(11)	28(4)
O(12)	165(13)	1323(15)	1368(7)	30(2)
O(13)	−1008(13)	−1165(16)	1194(7)	34(3)
C(20)	−4607(20)	1958(27)	−954(13)	44(5)
C(21)	−2911(19)	1218(22)	−630(10)	29(4)
O(22)	−1709(14)	2218(15)	−425(8)	34(3)
O(23)	−2831(13)	−277(14)	−541(7)	29(3)
Cl(3)	6219(5)	3621(6)	1562(3)	38(1)
O(31)	7236(15)	3829(22)	2458(8)	58(4)
O(32)	6747(18)	4716(19)	932(10)	60(4)
O(33)	6316(18)	1979(18)	1249(10)	55(4)
O(34)	4477(15)	4010(21)	1608(9)	57(4)

[a] U(eq) is defined as one-third of the trace of the orthogonalized U_{ij} tensor.

Table 3. Atomic Coordinates ($\times 10^4$) and Equivalent Isotropic Displacement Parameters ($Å^2 \times 10^3$) for the Non-Hydrogen Atoms in $[\{(H_2O)Pt(\mu\text{-}CH_3CO_2)_2\}_2](CF_3SO_3)_2\cdot 4H_2O$

	x	y	z	U(eq)[a]
Pt(1)	979(1)	651(1)	388(1)	30(1)
C(10)	1840(7)	−3960(6)	758(3)	52(2)
C(11)	1156(6)	−2532(6)	480(3)	39(1)
O(12)	1822(4)	−1334(4)	735(2)	40(1)
O(13)	−40(4)	−2572(3)	8(2)	38(1)
C(20)	−3296(7)	100(7)	1447(3)	48(1)
C(21)	−2092(6)	32(6)	923(2)	36(1)
O(22)	−694(5)	634(4)	1086(2)	41(1)
O(23)	−2534(4)	−577(4)	347(2)	39(1)
O(1)	2735(5)	1750(5)	1083(2)	45(1)
O(6)	−1286(7)	−1725(6)	2999(3)	61(1)
O(7)	4950(7)	−2150(7)	4619(3)	71(2)
S(81)	2536(2)	575(2)	3590(1)	42(1)
O(82)	1455(5)	1743(5)	3347(2)	65(1)
O(83)	3825(6)	1005(7)	4097(3)	86(2)
O(84)	1742(7)	−779(5)	3760(3)	82(2)
C(91)	3635(10)	70(9)	2866(3)	65(2)
F(92)	4414(7)	1208(6)	2623(3)	107(2)
F(93)	4776(7)	−961(6)	3036(3)	102(2)
F(94)	2641(9)	−404(7)	2343(2)	122(2)

[a] U(eq) is defined as one-third of the trace of the orthogonalized U_{ij} tensor.

significant differences in bond lengths or angles, except for the $Pt-OH_2$ distances (see below). Selected bond lengths and angles are listed in Table 4. Figure 2 shows the structure of the cation **1** in the triflate salt. With the metal−metal bond taken into account, each Pt atom shows approximately octahedral coordination. In each compound, the Pt′−Pt−O(acetate) angles are all slightly less than 90°, with an average of 88.1(3)°. This causes each Pt atom to be displaced 0.067(7) Å from the plane of the four acetate oxygen atoms coordinated to it.

The packing in the perchlorate salt is relatively simple, with each axially-coordinated water molecule (O(1)) interacting strongly with two oxygen atoms of the perchlorate anion (O(1)−O(34) 2.69(2) Å, O(1)−O(32) 2.74(2) Å). This interaction appears responsible for a slight bending of O(1) toward the perchlorate anion, so that the O(1)−Pt(1)−Pt(1)′ angle is slightly less than 180° (177.9(3)°). The packing in the triflate salt is more complex. There are hydrogen-bonding interactions between the water molecules bound to platinum and molecules of water of crystallization (O(1)−O(6) 2.62(1) Å, O(1)−O(7) 2.63(1) Å). Once again, there is a small deviation from linearity in the O(1)−Pt(1)−Pt(1)′ angle (178.6(1)°). There is a significant difference between the $Pt-OH_2$ bond lengths in the two salts (2.115(4) Å for the triflate, 2.177(13) Å for the perchlorate).

Table 4. Selected Bond Lengths and Angles for the Cation in $[\{(H_2O)Pt(\mu\text{-}CH_3CO_2)_2\}_2](ClO_4)_2$ and in $[\{(H_2O)Pt(\mu\text{-}CH_3CO_2)_2\}_2](CF_3SO_2)_2\cdot 4H_2O$[a]

	perchlorate	triflate		perchlorate	triflate
		Bond Lengths (Å)			
Pt(1)–Pt(1)′	2.3906(13)	2.3929(6)	Pt(1)–O(23)′	2.000(10)	2.000(3)
Pt(1)–O(1)	2.177(13)	2.115(4)	O(12)–C(11)	1.27(2)	1.283(6)
Pt(1)–O(12)	2.008(10)	2.004(3)	O(22)–C(21)	1.27(2)	1.275(6)
Pt(1)–O(13)′	2.002(10)	2.010(3)	O(13)–C(11)	1.27(2)	1.274(6)
Pt(1)–O(22)	2.023(11)	2.013(4)	O(23)–C(21)	1.24(2)	1.265(6)
		Bond Angles (deg)			
Pt(1)′–Pt(1)–O(1)	177.9(3)	178.6(1)	Pt(1)′–Pt(1)–O(13)′	88.7(4)	88.4(1)
O(1)–Pt(1)–O(12)	90.6(4)	90.6(2)	Pt(1)′–Pt(1)–O(22)	88.0(4)	88.0(1)
O(1)–Pt(1)–O(13)′	93.4(5)	93.0(2)	Pt(1)′–Pt(1)–O(23)′	88.0(4)	88.1(1)
O(1)–Pt(1)–O(22)	92.4(5)	92.1(2)	O(12)–C(11)–O(13)	126(1)	124.7(5)
O(1)–Pt(1)–O(23)′	91.7(5)	91.9(2)	O(22)–C(21)–O(23)	127(2)	125.1(5)
O(12)–Pt(1)–O(22)	92.1(4)	90.0(1)	Pt(1)–O(12)–C(11)	119.2(10)	119.8(3)
O(13)′–Pt(1)–O(22)	88.6(4)	90.3(1)	Pt(1)′–O(13)–C(11)	118.5(10)	119.2(3)
O(12)–Pt(1)–O(23)′	89.6(4)	89.4(1)	Pt(1)–O(22)–C(21)	117.6(11)	119.0(3)
O(13)′–Pt(1)–O(23)′	89.4(4)	90.1(1)	Pt(1)′–O(23)–C(21)	119.4(10)	119.8(3)
Pt(1)′–Pt(1)–O(12)	87.7(4)	87.9(1)			

[a] A prime indicates symmetry transformation used to generate equivalent atoms: $-x, -y, -z$.

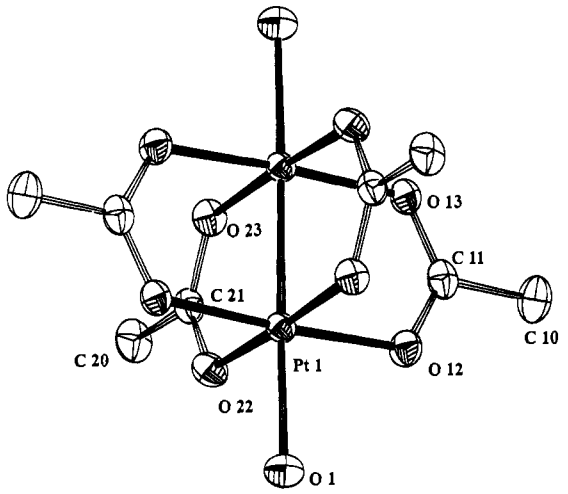

Figure 2. Platon diagram (30% probability ellipsoids) for the cation in $[\{(H_2O)Pt(\mu\text{-}CH_3CO_2)_2\}_2](CF_3SO_3)_2\cdot 4H_2O$.

Reaction of 1 with Water (Scheme 3). The ^1H NMR spectrum of **1** in D_2O would be expected to show a single peak, from the methyl protons of the bridging acetate ligands. When either the perchlorate or triflate salt was dissolved in D_2O, the ^1H NMR spectrum obtained as soon as possible (Figure 3a) showed that, on dissolution, **1** very rapidly reacted with the solvent. The spectra could be explained if the major product of this rapid reaction was **13**, in which one of the acetate bridges was broken. In **13**, two of the bridges are equivalent, giving the peak **b**. Peak **a** was assigned to the unique bridge, and **c** to the monodentate acetate. A much slower reaction then occurred over several hours (Figure 3b–d), in which the peaks from **13** decreased and a peak (**f**) from free acetate appeared, together with a new set of peaks (2:1 intensity, **e** and **d**; peak **e** coincident with **b** from **13**). Peaks **e** and **d** were assigned to **14**, in which the monodentate acetate has been replaced by water. The presence of a number of weaker peaks in the spectra (especially the initial spectrum, Figure 3a) indicated that there were also alternative decomposition routes for **1**. The solution containing **14** was relatively stable, with **14** still present after 24 h. A ^{195}Pt NMR spectrum of a solution containing **14** showed a singlet at 1320 ppm.

From the ratio of the peak heights for free acetate and reference TSS in ^1H NMR spectra, the liberation of acetate from **13** to give **14** could be followed. There was an excellent linear correlation between the logarithm of this ratio and time, indicating that the reaction followed first-order kinetics, with

Scheme 3

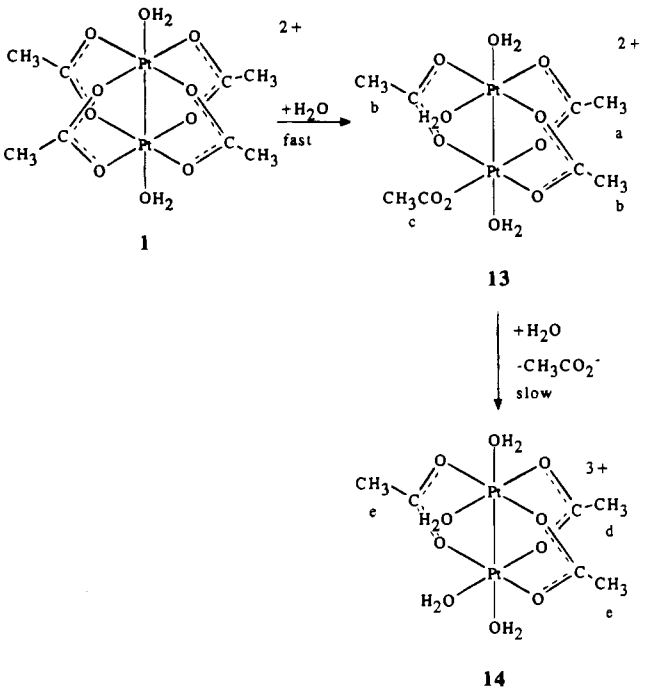

$k_{obs} = 3.3 \times 10^{-4}\ s^{-1}$ at 296 K, corresponding to a half-life close to 35 min. The same reaction was also followed by UV spectroscopy in a 6×10^{-5} M solution. The UV spectrum immediately after dissolution of $[\{(H_2O)Pt(\mu\text{-}CH_3CO_2)_2\}_2](ClO_4)_2$ in water showed a single peak with a broad maximum at 41 700 cm^{-1}, assigned to **13**, which slowly decreased with time. An excellent linear correlation was obtained between $\log(A - A_\infty)$ and time, where A is the absorbance at 40 000 cm^{-1}. The rate constant at 296 K was $3.65 \times 10^{-4}\ s^{-1}$, in good agreement with the value from NMR spectra.

Solutions in Acetic Acid. When the perchlorate or triflate salt $[\mathbf{1}]A_2$ was dissolved in either glacial acetic acid or a 3:1 (by volume) acetic acid/water mixture, a peak was observed in the ^{195}Pt NMR spectrum at 1520 ppm. The ^1H NMR spectrum in CD_3CO_2D or 3:1 CD_3CO_2D/D_2O showed a singlet at 2.48 ppm, with no resolved coupling to ^{195}Pt. These peaks were assigned to the complex with axial acetate ligands, $[\{(CH_3CO_2)Pt(\mu\text{-}CH_3CO_2)_2\}_2]$ (**9**). This species remained in solution for at least an hour, but slow decomposition did occur. After 5 h, the solution was blue. This color was probably due to the

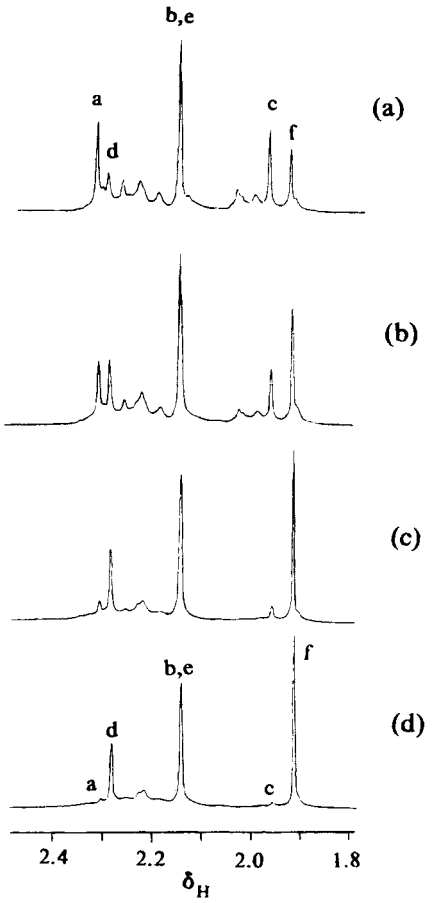

Figure 3. 200-MHz ^{1}H NMR spectra of a solution obtained by dissolving $[\{H_2O)Pt(\mu\text{-}CH_3CO_2)_2\}_2](ClO_4)_2$ in D_2O at (a) 5, (b) 17, (c) 77, and (d) 182 min after dissolution (at 298 K).

formation of oligomers with acetate-bridged platinum atoms in mixed II/III oxidation states (*cf.* "amide blues",[20] "phosphate blues" [21]).

Solutions in *N,N*-Dimethylformamide (dmf). The triflate salt, **[1]**$(CF_3SO_3)_2$, was very soluble in dmf (up to 0.3 M) (the perchlorate salt was almost insoluble). NMR spectra showed that the lantern structure retained its integrity for some time in this solvent, although dmf did, in part, replace the axial water ligands. The ^{195}Pt NMR spectrum of the solution showed four peaks (Figure 4), which were assigned on the basis of changes in relative intensities with time after dissolution in dmf (proportion with dmf coordinated increased), changes with concentration of the complex (proportion with dmf coordinated tended to increase with increased dilution), and changes when a small amount of water was added to the solution. A single peak at 1500 ppm was assigned to $[\{(dmf\text{-}O)Pt(\mu\text{-}CH_3CO_2)_2\}_2]^{2+}$ (**15**), a peak at 1456 ppm was assigned to $[\{(H_2O)Pt(\mu\text{-}CH_3CO_2)_2\}_2]^{2+}$ (**1**) in this solvent, and two peaks, at 1453 and 1450 ppm, were from isotopomers of $[(dmf)Pt(\mu\text{-}CH_3CO_2)_4Pt(H_2O)]^{2+}$ (**16**) with one ^{195}Pt nucleus present (weaker peaks expected from the isotopomer with two ^{195}Pt nuclei were too weak to be observed). The ^{1}H NMR spectrum in dmf-d_7 showed three singlets, assigned on a similar basis to the protons of the bridging acetate ligands of **15** (2.47 ppm), **16** (2.28 ppm), and **1** (2.07 ppm). With time, the ^{195}Pt peaks disappeared, and after 1 week, the ^{1}H NMR spectrum showed only a peak from free acetate at 1.97 ppm.

The 50.3-MHz ^{13}C NMR spectrum of the solution in dmf-d_7 showed two peaks, assignable to the methyl carbon (25.5 ppm) and carboxylate carbon (203.1 ppm) atoms. For neither peak was coupling to ^{195}Pt resolved. From the ^{1}H NMR spectrum of the solution, $[\{(dmf)Pt(\mu\text{-}CH_3CO_2)_2\}_2]^{2+}$ (**15**) was the dominant species present, so these ^{13}C peaks were assigned to **15**, with peaks from **16** and **1** either coincident or too weak to be observed.

Other Axially Substituted Complexes $[\{XPt(\mu\text{-}CH_3CO_2)_2\}_2]^{n+}$ and $[XPt(\mu\text{-}CH_3CO_2)_4PtY\}]^{n+}$. The solubility of **[1]**$(CF_3SO_3)_2$ in dmf and its relative stability in that solvent allowed the compounds with two axial halide ligands $[\{XPt(\mu\text{-}CH_3CO_2)_2\}_2]$ (X = Cl (**17**), Br (**18**)) to be prepared by reaction of **1** with the appropriate lithium halide in dmf. These compounds were only very sparingly soluble in water or chloroform. Once precipitated, they were slightly soluble in dmf but decomposed slowly in that solvent. The ^{1}H NMR spectrum of **17** in dmf-d_7 showed a singlet at 2.36 ppm from the methyl groups of the bridging acetate ligands, but within 30 min a peak from free acetate was also visible, which grew as the solution was allowed to stand. The yellow solid dichloro complex **17** was stable at ambient temperature, but the orange solid dibromo complex **18** decomposed over a period of weeks. The IR spectrum of each solid showed no bands in the O−H stretching region (*i.e.*, no water was present) and did show bands characteristic of bridging acetate (for **17**, ν_{as} 1558 cm^{-1}, ν_s 1417 cm^{-1}; for **18**, 1556 and 1416 cm^{-1}). A small amount of black solid (Pt metal?) deposited when LiBr was added to a dmf solution of **[1]**$(CF_3SO_3)_2$. If 1 mol equiv of LiI was added to a solution of **[1]**$(CF_3SO_3)_2$, there was immediate deposition of a black solid and liberation of I_2 into the dmf solution. Iodide ion caused similar reduction of the sulfate- and phosphate-bridged platinum(III) complexes.[13]

If the appropriate quantity of LiX was added to a relatively dilute solution of **[1]**$(CF_3SO_3)_2$ in dmf, precipitation of $[\{XPt(\mu\text{-}CH_3CO_2)_2\}_2]$ was slow and a ^{195}Pt NMR spectrum could be obtained if accumulation was commenced immediately. The dichloro complex **17** gave a ^{195}Pt NMR peak at 1447 ppm, and the dibromo compound **18** a peak at 990 ppm. If less than 2 mol equiv of LiCl was added, peaks were also observed due to $[ClPt(\mu\text{-}CH_3CO_2)_4Pt(dmf\text{-}O)]^+$ (**19**): peaks at 1572 and 1384 ppm, superimposed on an AB pattern from the isotopomer with two ^{195}Pt nuclei. The value of ^1J(Pt−Pt) measured from the spectrum was 5090 Hz.

The neutral ligands pyridine (py) or diethyl sulfide were also added to solutions of **[1]**$(CF_3SO_3)_2$ in dmf. No solids were isolated from these solutions, but ^{195}Pt NMR spectra of the dmf solutions provided the following values of δ_{Pt}: $[\{(py)Pt(\mu\text{-}CH_3CO_2)_2\}_2]^{2+}$ (**20**), 1398 ppm; $[(py)Pt(\mu\text{-}CH_3CO_2)_4Pt(dmf)]^{2+}$ (**21**), 1374 and 1242 ppm; $[\{(Et_2S)Pt(\mu\text{-}CH_3CO_2)_2\}_2]^{2+}$ (**22**), 1200 ppm; $[(Et_2S)Pt(\mu\text{-}CH_3CO_2)_4Pt(dmf)]^{2+}$ (**23**), 1265 and 1388 ppm. For the unsymmetrical complexes **21** and **23**, the peaks of the AB pattern from the isotopomer with two ^{195}Pt nuclei were not sufficiently intense to allow measurement of the Pt−Pt coupling constant. Attempts to obtain complexes with axial nitrite or thiocyanate were unsuccessful because of decomposition of the platinum(III) compounds.

Solid-State ^{13}C NMR Spectra. Because of the low solubilities of the salts of **1** in most solvents and their limited stabilities in solution, solid-state ^{13}C NMR spectra were obtained for **[1]**$(CF_3SO_3)_2$ and the dichloro complex **17**, as well as, for comparison, $[\{(H_2O)Rh(\mu\text{-}CH_3CO_2)_2\}_2]$. Apart from spinning sidebands (and, for the triflate salt, weak peaks from the CF_3^- group), each spectrum showed two peaks, from the methyl and carboxylate C atoms of the bridging acetate ligands. Figure 5 shows the spectrum obtained for the triflate salt. Shifts are listed in Table 5.

UV Spectra. The solvents which were available for record-

(20) Lippard, S. J. *Acc. Chem. Res.* **1978**, *11*, 211.
(21) Appleton, T. G.; Berry, R. D.; Hall, J. R. *Inorg. Chim. Acta* **1982**, *64*, L229.

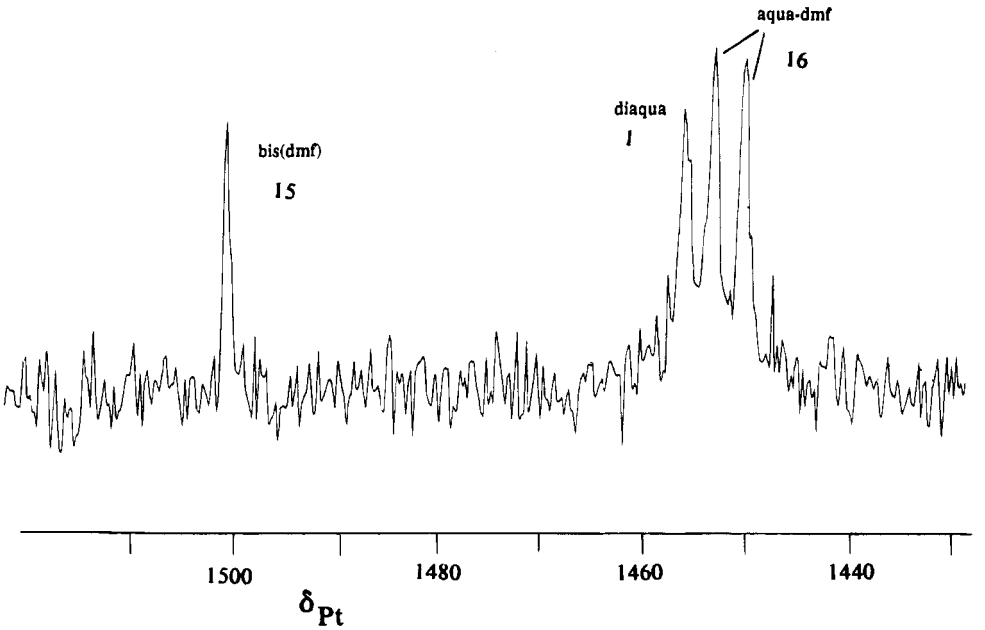

Figure 4. 21.4-MHz ^{195}Pt NMR spectrum of a solution of $[\{(H_2O)Pt(\mu\text{-}CH_3CO_2)_2\}](CF_3SO_3)_2$ in dmf. Labels refer to the axial ligands.

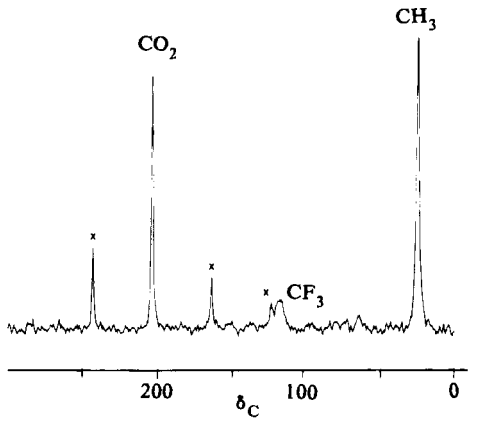

Figure 5. ^1H-decoupled CP-MAS 75.5-MHz ^{13}C NMR spectrum of solid $[\{(H_2O)Pt(\mu\text{-}CH_3CO_2)_2\}](CF_3SO_3)_2$. × = spinning sideband.

Table 5. ^{13}C NMR Shifts for Tetra-Acetate-Bridged Complexes

compound	medium	δC carboxylate	δC methyl
$[\{(H_2O)Rh(\mu\text{-}CH_3CO_2)_2\}_2]^a$	D_2O	194.8	31.4
	solid	192.6	23.9
$[\{(H_2O)Pt(\mu\text{-}CH_3CO_2)_2\}_2](CF_3SO_3)_2$	solid	203.5	25.0
$[\{(dmf\text{-}O)Pt(\mu\text{-}CH_3CO_2)_2\}_2](CF_3SO_3)_2$	dmf-d_7	203.1	25.5
$[\{ClPt(\mu\text{-}CH_3CO_2)_2\}_2]$	solid	203.2	26.3

[a] Shifts relative to internal dioxane, taken as 67.73 ppm.

ing UV spectra were determined by the solubility and stability factors previously discussed. Since decomposition occurred at least slowly in all solvents, solution spectra were run as soon as possible after dissolution. Solution spectra were obtained for $[\{(CH_3CO_2)Pt(\mu\text{-}CH_3CO_2)_2\}_2]$ (**9**), from a solution of **[1]**$(CF_3SO_3)_2$ in glacial acetic acid, for $[\{XPt(\mu\text{-}CH_3CO_2)_2\}_2]$ (X = Cl (**17**), Br (**18**)) in dmf, and for a solution of **[1]**$(CF_3SO_3)_2$ in dmf. The latter solution would contain a mixture of complexes with axial dmf and H_2O ligands although, in the dilute solution used, $[\{(dmf\text{-}O)Pt(\mu\text{-}CH_3CO_2)_2\}_2]^{2+}$ (**15**) would predominate. The spectrum was also obtained for a Nafion film dipped in a dmf solution (see Experimental Section). Although **15** would have predominated in the solution, it is possible that the relative populations of cations adsorbed on the film surface could differ from that in the solution. The spectrum of this

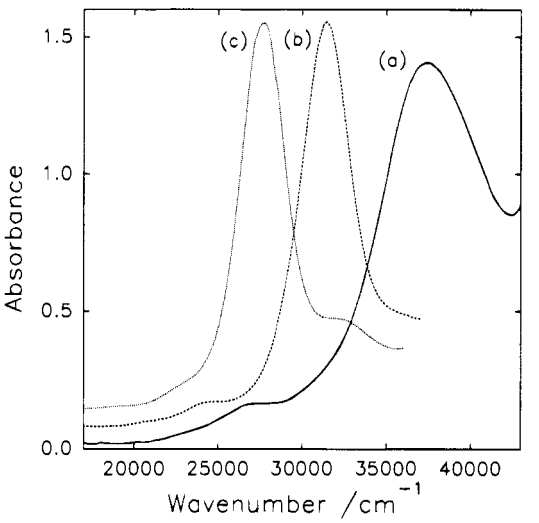

Figure 6. Electronic absorption spectra: (a) Nafion film dipped for 1 s in 10^{-2} M solution of $[\{(H_2O)Pt(\mu\text{-}CH_3CO_2)_2\}_2](CF_3SO_3)_2$ in dmf (292 K); (b) 6×10^{-5} M $[\{ClPt(\mu\text{-}CH_3CO_2)_2\}_2]$ in dmf; (c) 5×10^{-5} M $[\{BrPt(\mu\text{-}CH_3CO_2)_2\}_2]$ in dmf.

Nafion film and the spectra of **17** and **18** in dmf solution are shown in Figure 6.

Each spectrum showed a very strong band in the near UV (band B, $\epsilon_{max} > 15\,000$) and a much weaker band to lower energy (band A, $\epsilon_{max} < 3000$). For the dibromo complex, **18**, an additional weak band (band C) was observed to higher energy from band B. Details are listed in Table 6.

For the complexes with two halide ligands, **17** and **18**, the UV bands all decreased in intensity with time. Good linear correlations were obtained between $\log(A - A_\infty)$ at a particular wavelength and time. First-order rate constants for decay of the complexes at 296 K were $(1.4 \pm 0.2) \times 10^{-4}$ s^{-1} for **17** and $(0.9 \pm 0.1) \times 10^{-4}$ s^{-1} for **18**.

Discussion

Formation of 1 in the Reaction of $[Pt(NO_2)_4]^{2-}$ with CH_3CO_2H/HA/H_2O. From comparison with our previous results,[14] it is evident that the presence of the strong acid HA together with CH_3CO_2H in the reaction with $[Pt(NO_2)_4]^{2-}$ makes possible the formation of **1**. As well as removing the final nitrite ligands from the platinum(III) compound $[\{LPt(NO_2)\}_2$-

Table 6. UV Spectroscopic Data[a]

	band A $\pi^*(Pt_2) \rightarrow \sigma^*(Pt_2)$		band B $\sigma(X) \rightarrow \sigma^*(Pt_2)$		band C $\pi(Pt_2) \rightarrow \sigma^*(Pt-O)$	
axial ligand	posn (cm^{-1})	ϵ_{max}	posn (cm^{-1})	ϵ_{max}	posn (cm^{-1})	ϵ_{max}
dmf[b]	25 000	1500	37 000[d]	18 000[d]	*c*	
dmf[b,e] (292 K)	27 000		37 300			
dmf[b,e] (10 K)	27 300		37 600			
$CH_3CO_2^-$	27 000	2000	34 200	13 000	*c*	
Cl^-	24 300	2000	31 400	23 000	*c*	
Br^-	22 700	2000	27 700	28 000	32 700	7000

[a] Molar extinction coefficients reported for solution spectra are approximate only due to gradual decomposition of these compounds. [b] Complexes with axial H_2O may also be present—see text. [c] Not observed. [d] Approximate value; band partly obscured by solvent absorption. [e] Nafion film dipped in 10^{-2} M solution in dmf.

$(\mu\text{-}CH_3CO_2)_3]^{n-}$ (**8a,b**), which is the final reaction product in aqueous acetic acid,[14] the strong acid will affect the reactions occurring in many other ways. It will decrease the proportion of acetate present relative to acetic acid. This will tend to hinder the formation of acetate complexes essential for the reaction to proceed, but this is outweighed by other effects. It will also affect the competition between nitrite removal and Pt(II) oxidation in the early stages of the reaction. Nitrite removal from Pt(II) will be more efficient. The much lower amounts of Pt(IV) complexes produced when HA was present may be related to the much faster disappearance of the tetra- and trinitritoplatinum(II) mononuclear complexes which are oxidized most readily to Pt(IV). There will be higher concentrations of nitrate present in the early stages of the reaction, and the oxidation potential of the nitrate will also be affected by the higher H^+ ion concentration. As illustrated in Schemes 1 and 2, intermediate Pt(III) compounds under oxygen with HA present are different from those formed under argon and are also different from those present under similar conditions without HA.[14]

Electronic Spectra of $[\{XPt(\mu\text{-}CH_3CO_2)_2\}_2]^{n+}$. The spectra in Figure 6, with intense band B and weaker band A, are similar to those observed for other tetrabridged d^7–d^7 metal–metal σ-bonded dimers, including the rhodium(II) analogues.[6,22-33] In comparing platinum(III) with rhodium(II) compounds, one should realize that the higher charge on platinum will stabilize the 5d orbitals, resulting in greater mixing of the metal d orbitals with the ligand orbitals as well as lower energy LMCT transitions. The band positions and relative intensities are very similar to those reported recently for the closely-related complexes $[\{XPt(\mu\text{-}SO_4)_2\}_2]^{m-}$ and $[\{XPt(\mu\text{-}HPO_4)_2\}_2]^{m-}$ (X = H_2O, Cl, Br).[31-33] The electronic structures of these two dimer systems have been probed by low-temperature polarized single-crystal absorption,[32] emission,[31,32] and, very recently, MCD[33] spectroscopy. Due to the close similarity of the spectra of the acetate complexes to those of the sulfate and phosphate dimer complexes, analogous spectral assignments should apply.

As seen from Table 6 and Figure 6, band B exhibits the characteristic lower energy shift when the axial ligands are changed from H_2O/dmf to $CH_3CO_2^-$, Cl^-, and then Br^-, indicating that at least one of the orbitals involved in the transition has significant axial ligand character.[31,32] Previously, the analogous band in Pt(III) dimeric complexes has been assigned to the $\sigma(X) \rightarrow \sigma^*(Pt_2)$ transition corresponding to the *z*-polarized $a_{1g} \rightarrow a_{2u}$ spin-allowed transition. However, the recent MCD analysis of the sulfate and phosphate complexes[33] is in conflict with this assignment, as an MCD *A* term was observed for this band, indicating a transition to an orbitally degenerate excited state. In fact, the sign of the *A* term for this band differed when the axial ligands were changed from H_2O to Cl^-, implying that different excited states are involved for these two complexes. For consistency with the observed MCD, this band was tentatively assigned to a LMCT transition from the bridging oxygen atoms for the diaqua complex and to a π-LMCT transition from the axial halide ligands for the dihalo complexes.

However, some caution is necessary in the interpretation of the MCD spectra for the sulfate and phosphate complexes, as quite strong MCD *A* and *B* terms were also observed in regions of the spectrum where there was little or no absorption. The *A* terms assigned to the intense near-UV band (band B) may therefore actually be associated with other, relatively weak, absorptions coincident with or close to this band. If band B does not correspond to the $\sigma(X) \rightarrow \sigma^*(Pt_2)$ transition, then where does this transition lie? In the related complex with the pyrophosphite ligand, $P_2O_5H_22-$ (pop^{2-}), $[\{BrPt(\mu\text{-}pop)_2\}_2]^{4-}$, the $\sigma(X) \rightarrow \sigma^*(Pt_2)$ transition occurs near 32 000 cm^{-1},[30] and although the Pt–Pt distance is longer for the pop complex, it is unlikely that the same transition in the phosphate and sulfate complexes would lie very much higher in energy. A temperature-dependent MCD study of these systems is desirable to elucidate the competing effects of *A* and *B* MCD terms. It is more than likely, however, that band B involves contributions from both the $\sigma(X) \rightarrow \sigma^*(Pt_2)$ and LMCT transitions.

The weaker band (band A) to the lower energy side of band B in the spectra of $[\{XPt(\mu\text{-}CH_3CO_2)_2\}_2]^{n+}$ is less sensitive to changes in axial ligation. In the analogous sulfate, phosphate, and pop complexes, this band was assigned to the *x,y*-polarized $\pi^*(Pt_2) \rightarrow \sigma^*(Pt_2)$ ($e_g \rightarrow a_{2u}$) spin-allowed transition.[30-33] The decreased sensitivity to the axial ligands is expected for this transition, as the $\pi^*(Pt_2)$ orbitals contain negligible axial ligand character. Unfortunately, the limited solubility of the complexes did not permit the observation of the very weak spin-triplet $\pi^*(Pt_2) \rightarrow \sigma^*(Pt_2)$ transition expected to lie between 3000 and 5000 cm^{-1} to lower energy from the spin-allowed $\pi^*(Pt_2) \rightarrow \sigma^*(Pt_2)$ transition.[31,32]

For the dibromo complex **18**, an additional weak band, band C, was observed near 32 000 cm^{-1}, on the higher-energy side of the intense band B. A similar band was also observed for the analogous sulfate and phosphate complexes but was not assigned.[31,32] For the phosphate complex, a negative MCD *A* term was observed for this band, which is consistent with assignment as the *x,y*-polarized $\pi(Pt_2) \rightarrow \sigma^*(Pt-O)$ ($e_u \rightarrow b_{1g}$) spin-allowed transition. We recently undertook SCF–Xα–SW electronic structure calculations on these Pt(III) dimeric systems in order to obtain a reasonable picture of the one-electron orbital sequence and approximate transition energies.[34]

(22) (a) Wilson, C. R.; Taube, H. *Inorg. Chem.* **1975**, *14*, 405. (b) *Inorg. Chem.* **1975**, *14*, 2276.
(23) Miskowski, V. M.; Schaefer, W. P.; Sadeghi, B.; Santarsiero, B. D.; Gray, H. B. *Inorg. Chem.* **1984**, *23*, 1154.
(24) Miskowski, V. M.; Gray, H. B. In *Understanding Molecular Properties*; Avery, J., Dahl, J. P, Eds; Reidel: Dordecht, The Netherlands, 1987; pp 1–16.
(25) Roundhill, D. M.; Gray, H. B.; Che, C.-M. *Acc. Chem. Res.* **1989**, *22*, 55.
(26) Zipp, A. P. *Coord. Chem. Rev.* **1988**, *84*, 47.
(27) Che, C.-M.; Mak, T. C. W.; Miskowski, V. M.; Gray, H. B. *J. Am. Chem. Soc.* **1986**, *108*, 7840.
(28) Che, C.-M.; Butler, L. G.; Grunthaner, P. J.; Gray, H. B. *Inorg. Chem.* **1985**, *24*, 4662.
(29) Che, C.-M.; Lee, W.-M.; Cho, K.-C. *J. Am. Chem. Soc.* **1988**, *110*, 5407.
(30) Isci, H.; Mason, W. R. *Inorg. Chem.* **1985**, *24*, 1761.
(31) Shin, Y.-K.; Miskowski, V. M.; Nocera, D. G. *Inorg. Chem.* **1990**, *29*, 2308.
(32) Newman, R. A.; Martin, D. S.; Dallinger, R. F.; Woodruff, W. H.; Stiegman, A. E.; Che, C.-M.; Schaefer, W. P.; Miskowski, V. M.; Gray, H. B. *Inorg. Chem.* **1991**, *30*, 4647.
(33) Gokagac, G.; Isci, H.; Mason, W. R. *Inorg. Chem.* **1992**, *31*, 2184.

Evidence for Strain in the Tetra-Acetate-Bridged Structure. As mentioned in the description of the crystal structures of the salts of **1** above, the Pt−Pt−O(acetate) angles in both the perchlorate and triflate salts are all slightly less than 90°, with an average of 88.1(3)°, so that each Pt atom is displaced 0.067(7) Å out of the plane of the four acetate O atoms bound to it. These deviations from 90° are small, but since they are present in the two salts with very different crystal packing, they are certainly reproducible. We suggested in our previous communication[1] that the very short Pt−Pt distance (average 2.392 Å) in **1** is due to the constraints imposed by the tetra-acetate-bridged structure, so that there is repulsion between the Pt atoms and strain in the structure. We noted that, in the much more robust sulfate analogue $K_2[\{(H_2O)Pt(\mu\text{-}SO_4)_2\}_2]$, the average Pt−Pt−O(sulfate) angle is 89.9(1)°, with the Pt−Pt distance 2.461(1) Å, which we suggested is close to optimum for a platinum(III) complex with O-donor ligands.[9] In the hydrogen phosphate analogue, the average Pt−Pt−O(phosphate) angle is slightly greater than 90°, 90.8(1)°, with a slightly longer Pt−Pt bond length, 2.487(2) Å.[9]

The angles and bond lengths within the bridging acetate groups of **1** are not significantly different from those in $K_2[\{Pt(NO_2)_2(\mu\text{-}CH_3CO_2)\}_2]\cdot 0.5H_2O$.[14] The C−O−Pt angles in this Pt(II) complex (ranging from 123.5(12) to 126.5(10)°, average 124.8°) are, as would be expected, larger than the corresponding angles in the salts of **1** (ranging from 117.6(11) to 119.8(3)°, average 118.8°).

The ^{13}C NMR results listed in Table 5 for the tetra-acetate-bridged platinum complexes for spectra obtained both in solution and in the solid state showed that the carboxylate carbon nucleus was remarkably deshielded, with shifts close to 203 ppm. This may be compared with shifts for monodentate coordinated acetate (183.5 ppm in *cis*-$[Pt(NH_3)_2(-O_2CCH_3)(H_2O)]^+$ [35]) and nonstrained bridging acetate (179.6 ppm in the platinum(III) complex with two acetate bridges $[\{(mepy)Pt(CH_3)_2(\mu\text{-}CH_3CO_2)\}_2]$[36]). For the unusual organometallic platinum(III) complex **24**, the two carboxylate ^{13}C shifts reported were 189.1 and 190.4 ppm.[37] Although the different resonances were not assigned, it is evident that the shift for the "normal" bridging acetates in **24** is close to 190 ppm. We propose that the exceptional deshielding in **1** and its derivatives is a result of strain in the acetate bridges.

We noted previously[1] that **1** was structurally very similar to rhodium(II) acetate, with a similar metal−metal bond length (Rh−Rh 2.3855(5) Å[5]) and with similar small angular distortions (average Rh−Rh−O angle 88.1(3)°, with Rh displaced 0.069(2) Å from the O_4 plane). We suggested that this is also a strained system, although chemically much more robust than the tetra-acetate-bridged platinum(III) analogues. The ^{13}C shifts listed in Table 5 for rhodium(II) acetate in the solid state and in aqueous solution showed that the carboxylate carbon was deshielded compared with "normal" coordinated acetate in the examples given above, but much more shielded than for **1**. If strain is the source of unusually low shielding, then the bridges in the rhodium compound are strained, but less so than in the Pt(III) complexes, consistent with the greater chemical stability of the rhodium compound. The value for carboxylate δ_C would then be a more sensitive indicator of strain than the internal acetate angles obtained through X-ray diffraction.

^{195}Pt NMR Parameters. Since all of the Pt(III) "lantern" complexes for which structures have been determined have been symmetrical, values of J(Pt−Pt) are not available for compounds for which crystal structures are available. However, with the assumption that Pt−Pt bond lengths would follow the same trend as bridging ligands are changed as for symmetrical complexes, we previously noted[13] that values of J(Pt−Pt) for phosphate-bridged compounds, expected to have slightly longer Pt−Pt bond lengths, were larger than those for corresponding sulfate-bridged compounds. For example, J(Pt−Pt) for $[ClPt(\mu\text{-}HPO_4)_4Pt(OH_2)]^{3-}$ is 5342 Hz and that for $[ClPt(\mu\text{-}SO_4)_4Pt(OH_2)]^{3-}$ 3464 Hz.[13] If the reasonable assumption is made that the trans influence of O-bound dmf is not very different from that of H_2O, these values may be compared with that for $[ClPt(\mu\text{-}CH_3CO_2)_4Pt(dmf\text{-}O)]^+$ (**19**), 5090 Hz. Despite the much shorter Pt−Pt distance expected for the compound with acetate bridges, the coupling constant is slightly less than for the phosphate complex!

The changes in δ_{Pt} when the axial ligands were changed in the acetate-bridged complexes followed the same order as for the sulfate and phosphate complexes previously studied.[13] By analogy with the assignments previously made for the sulfate and phosphate chloro aqua compounds, the more shielded Pt nucleus (δ_{Pt} 1384) in $[ClPt(\mu\text{-}CH_3CO_2)_4Pt(dmf\text{-}O)]^+$ (**19**) was assigned as that to which chloride is bound (with δ_{Pt} for Pt(dmf) 1572). Although the absolute values of δ_{Pt} are different for the three different bridging ligands, the chemical shift differences for the two nonequivalent Pt atoms in each of these three species are quite similar (188 ppm for **19**, 170 ppm for $[ClPt(\mu\text{-}SO_4)_4Pt(OH_2)]^{3-}$, and 173 ppm for $[ClPt(\mu\text{-}HPO_4)_4Pt(OH_2)]^{3-}$ [13]).

Bonds to Axial Water Ligands. The major difference between the structures of the cation **1** in the perchlorate and triflate salts is in the Pt−OH_2 distances for the axial water ligands, 2.177(13) and 2.115(4) Å, respectively. The major difference between these structures of **1** and that of $[\{(H_2O)Rh(\mu\text{-}CH_3CO_2)_2\}_2]$ is, again, in the M−OH_2 distance, a very long 2.310(3) Å for the rhodium compound.[5] The Pt−OH_2 distances for the Pt(III) sulfate and phosphate, with longer Pt−Pt bonds than in **1**, are 2.111(7) and 2.16(1) Å, respectively. The differences in M−OH_2 bond lengths appear to be caused primarily by H-bonding and other intermolecular interactions. The large variations indicate that the axial M−OH_2 bonds are probably quite weak, with variation in the M−O distance causing little change in bond energy. Clearly, there is no correlation between M−OH_2 and M−M bond lengths.

Acknowledgment. We thank the Australian Research Council for financial support and Dr. A. Whittaker, of the Centre for Magnetic Resonance at this university, for providing solid-state NMR spectra.

Supporting Information Available: Tables listing experimental crystallographic details, anisotropic thermal parameters, positional parameters for hydrogen atoms, and all bond lengths and angles for both compounds and a figure showing crystal packing in the trifluoromethanesulfonate (7 pages). Ordering information is given on any current masthead page.

IC950169R

(34) Stranger, R.; Medley, G. A.; McGrady, J. E.; Garrett, J. M.; Appleton, T. G.; Heath, G. A. Submitted for publication.
(35) Appleton, T. G.; Berry, R. D.; Davis, C. A.; Hall, J. R.; Kimlin, H. A. *Inorg. Chem.* **1984**, *23*, 3514.
(36) Kuyper, J.; Vrieze, K. *Transition Met. Chem.* **1976**, *1*, 208.
(37) Yamaguchi, T.; Sasaki, Y.; Ito, T. *J. Am. Chem. Soc.* **1990**, *112*, 4038.